Analysis of aerodynamic and aeroacoustic behaviour of a simplified high-speed train bogie

J.Y. Zhu[1], **Z.W. Hu**[1], **D.J. Thompson**[2]

[1] Aerodynamics and Flight Mechanics Research Group, Faculty of Engineering and the Environment, University of Southampton, Southampton SO17 1BJ, UK

[2] Institute of Sound and Vibration Research, Faculty of Engineering and the Environment, University of Southampton, Southampton SO17 1BJ, UK

E-mail: jz1e10@soton.ac.uk, z.hu@soton.ac.uk, djt@isvr.soton.ac.uk

Summary

As one of the main aerodynamic noise sources of high-speed trains, the bogie is a complex structure containing many components and the flow around it is extremely dynamic with high-level turbulence. Flow around a simplified bogie at scale 1:10 is studied numerically using Computational Fluid Dynamics (CFD) for comparison with experimental measurements. The upstream inlet flow is represented as a steady uniform flow of low turbulence level in the simulations. Following a rigorous grid refinement study, multi-block fully structured meshes with hexahedral cells are generated for all cases to improve numerical efficiency and accuracy. The aerodynamic and aeroacoustic behaviour of the flow past an isolated wheelset, tandem wheelsets and a simplified bogie are investigated.

1 Introduction

For high-speed trains, aerodynamic noise becomes significant when the trains run above 300 km/h and can become predominant at higher speeds or with the reduction of the rolling noise [1, 2]. The aeroacoustic behaviour of high-speed trains needs further study, especially numerical investigations which can reveal more information on the flow physics. The prediction of aerodynamic noise in an industrial context is still very difficult to achieve due to the large computational resources required for unsteady numerical simulations [3]. The aim of this paper is to study the flow behaviour and the aerodynamic noise generation and radiation mechanisms from a simplified bogie using CFD. The Delayed Detached-Eddy Simulation (DDES) turbulence model [4] is used together with the Ffowcs Williams-Hawkings (FW-H) acoustic analogy method for radiated sound prediction [5]. DDES is developed to avoid grid-induced separation and preserve the Reynolds-Averaged Navier-Stokes (RANS) mode throughout the boundary layer [4]. The work commences with the flow behaviour and aeroacoustic characteristics around an isolated wheelset before progressing to tandem wheelsets

and then a simplified bogie model. The 1:10 scale case of simplified geometry is modeled with inlet velocity of 30 m/s for comparison with wind tunnel tests.

2 Numerical Setup

The configuration of the simplified bogie is displayed in Fig. 1. Generally, the wheel-mounted braking systems are implemented in the power bogie of high-speed trains. Thus, the wheel may be represented as a disc by neglecting the flange of the running surface and the gap between the wheel and braking discs. The isolated wheelset and tandem wheelsets have the same geometry as the simplified bogie by removing the frame. As a main part of the wheelset, the axle is a typical circular cylinder. Thus, the influence of mesh resolution is investigated based on the flow simulated around a circular cylinder. Considering the computer ability and computation efficiency, a structured mesh based on the baseline grids is generated for simulation. The distance from the wall surface to the nearest grid point is set as 10^{-5} m and stretched with a growth ratio of 1.1 inside the boundary layer, yielding a maximum value of y^+ (this dimensionless first-cell spacing is based on the viscosity and wall shear stress of a flow) less than 1 in most areas which is adequate for the low-Reynolds number turbulence model being used. The final mesh used for the isolated wheelset model has 5.3 million grid points and 14.5 million is applied for the simplified bogie case. The physical timestep size is 10^{-5} s to ensure sufficiently small Courant-Friedrichs-Lewy (CFL) value of less than 2 for most of the computational domain, indicative of adequate temporal resolution for the simulation to be converged at each timestep. CFD calculations have been performed using the open source software OpenFOAM®.

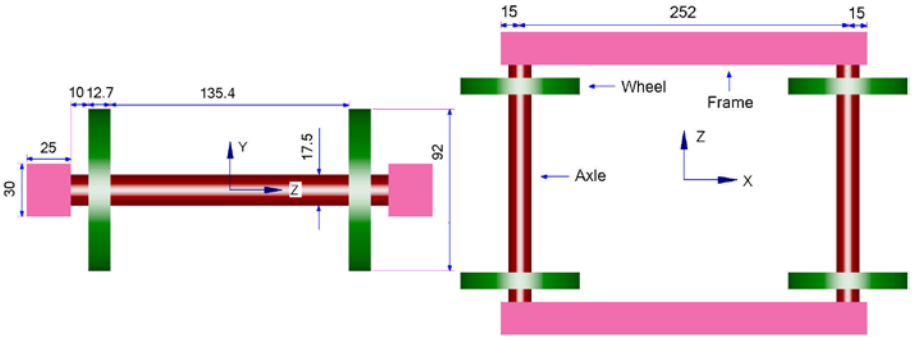

Fig. 1. Simplified bogie model (1:10 scale, dimensions in millimetres)

3 Aerodynamic Results

For isolated wheelset case, Fig. 2 visualizes the flow structures represented by the isosurfaces of normalized second invariant of velocity gradient Q (at level of 50) and coloured by the velocity magnitude. It can be seen that the flow past the

isolated wheelset is characterized by considerable coherent alternating vortex shedding with different sizes and orientations. The incoming inflow separates and reattaches on the wheel flat side surface where a crescent-shaped separation bubble appears and the horseshoe-shaped eddies are formed and convected downstream as two streamwise pairs of counter-rotating eddies. The flow separation and vortex shedding are also generated in the wake area.

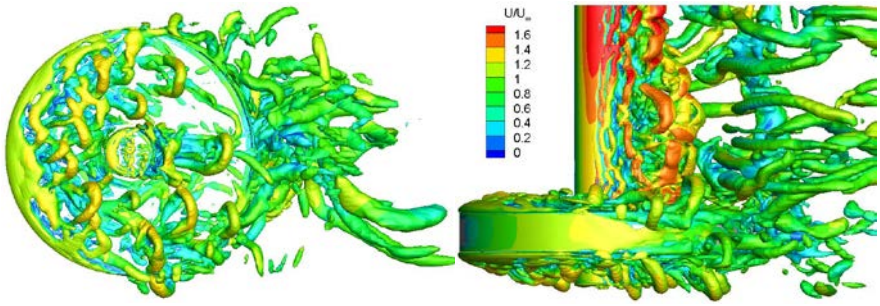

Fig. 2. Isosurface of the instantaneous normalized *Q* criterion (left: side view; right: top view)

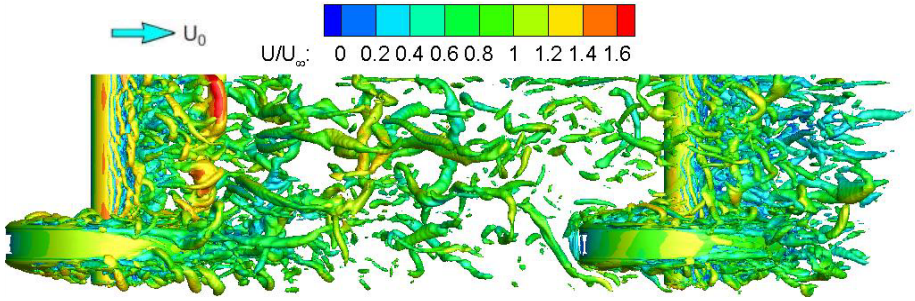

Fig. 3. Isosurface of the instantaneous normalized *Q* criterion (top view)

Fig. 3 shows the wake structure for the tandem wheelsets. This shows that the vortices are shed from the upstream wheelset, impinge on the downstream wheelset, deform largely and are merged into the eddies formed behind the rear wheelset, making the wake of the downstream wheelset highly turbulent.

The instantaneous non-dimensional spanwise vorticity fields (ω_Z) in the front and rear axle wake area of tandem wheelsets are displayed in Fig. 4. It also can be noted that the vortices shed alternately from the upstream axle impinge on the downstream axle and all vortices are mixed up behind the rear axle, leading to the synchronized behaviour of the downstream axle wake.

The wake structure for the simplified bogie is visualized in Fig. 5. Different with the tandem wheelsets case, the streamwise ‘rib’ vortices from the upstream axle between the wheels are distributed obliquely along the streamline direction since the turbulent flow develops more quickly close to the mid-span axle region as there is much less blockage far away from the wheel-frame area.

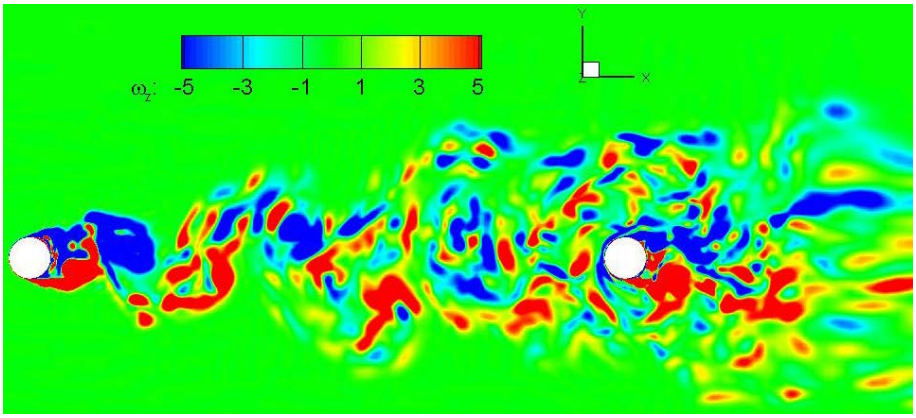

Fig. 4. Contours of instantaneous spanwise vorticity fields in vertical plane through centre of axle

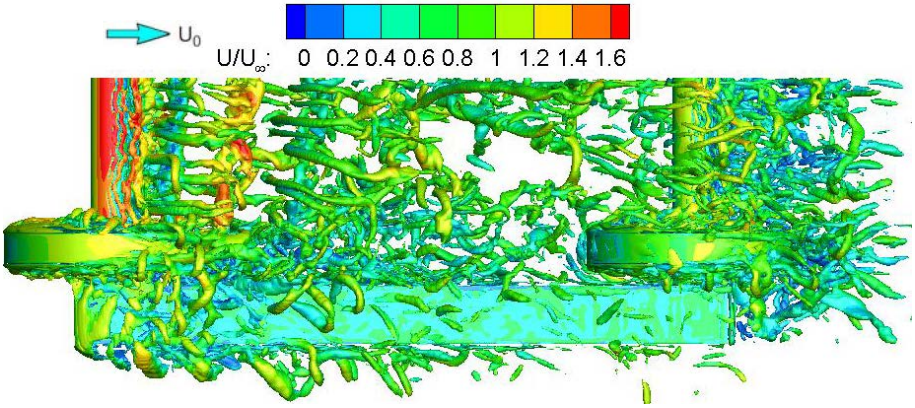

Fig. 5. Isosurface of the instantaneous normalized *Q* criterion (top view)

4 Aeroacoustic Results

Based on the near-field unsteady flow data obtained from the CFD calculations, the FW-H method can predict sound generation by equivalent acoustic sources such as monopoles, dipoles, and quadrupoles [5, 6]. The power spectral density (PSD) of the sound pressure is computed by segmental average (50% overlap) using a Hanning window applied to each segment with a frequency resolution of 6 Hz. The noise directivity is obtained based on Overall Sound Pressure Level (OASPL) calculated at the frequency range below 5 kHz. The receivers are distributed uniformly on a circular frame with radius 2.5 m at an interval of 5º to measure the noise directivity from the wheelset centerline along the vertical Y-Z plane and horizontal X-Z plane as represented in Fig. 1.

For isolated wheelset case, Fig. 6 shows the spectra of the noise radiated from the wheel and the axle separately at the top microphone position and Fig. 7 from the whole wheelset. Tonal noises are found with dominant frequencies at 311 Hz (with a Strouhal number *St* of 0.18 based on the axle diameter) and 622 Hz (*St* of 0.36) corresponding to the periodic vortex shedding around the axle and the wheel respectively. The sound radiation generated from the wheel in the presence of the axle is mainly associated with the oscillating drag forces exerted back on the fluid around the wheelset, whereas the noise generation from the axle mainly corresponds to the oscillating lift forces. As is well known, the aerodynamic forces acting in the vertical direction fluctuate with larger amplitude at half the frequency of those along the streamwise direction. At full scale these peaks would occur at 1/10 of these frequencies, but would increase with flow speed.

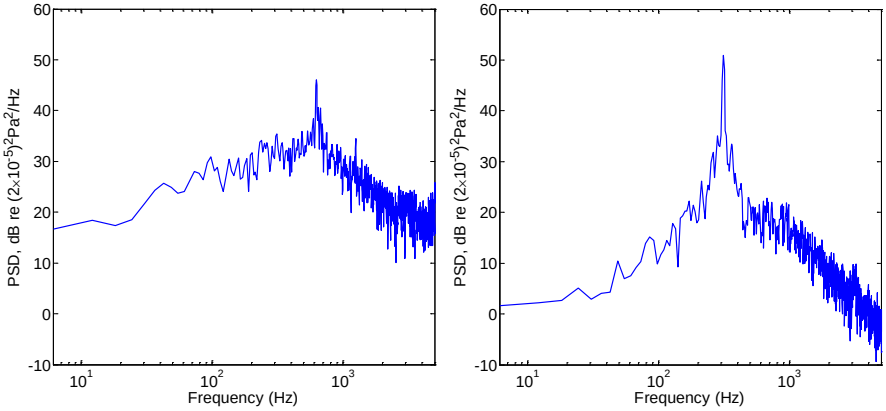

Fig. 6. Spectra computation of the radiated noise (left: wheel; right: axle)

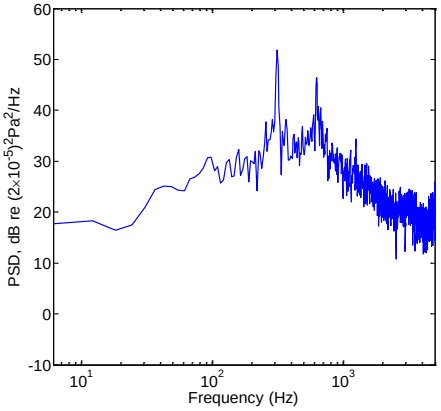

Fig. 7. Spectra of noise from whole wheelset

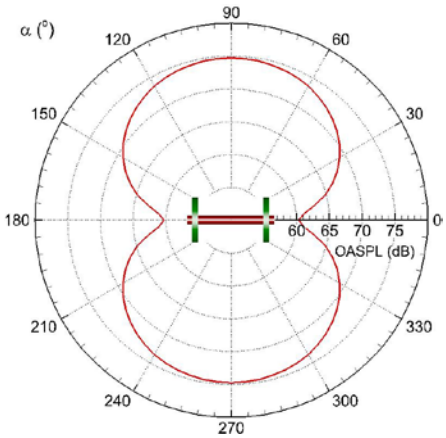

Fig. 8. Noise directivity from isolated wheelset (vertical Y-Z plane)

Fig. 8 shows the noise directivity radiated from the isolated wheelset in the vertical Y-Z plane normal to the flow direction (in this plane, the angle α=0º or 180º corresponds to the side of the train). This reveals that a typical dipole sound is generated by the flow separation from the wheelset top/bottom surfaces and radiates predominantly in the vertical direction.

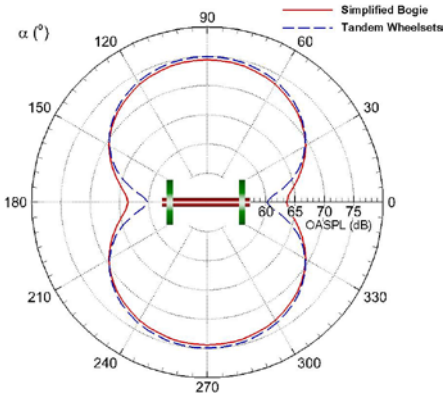

Fig. 9. Noise directivity from front wheelset (vertical Y-Z plane)

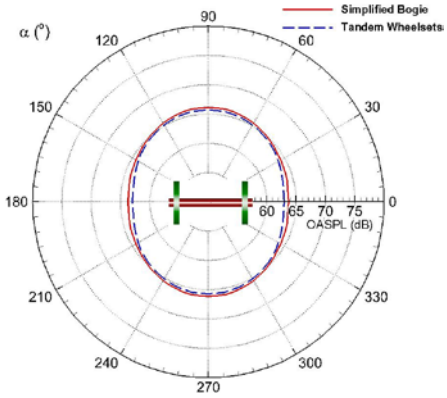

Fig. 10. Noise directivity from rear wheelset (vertical Y-Z plane)

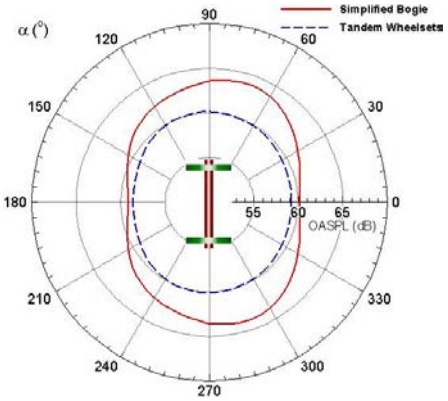

Fig. 11. Noise directivity from front wheelset (horizontal X-Z plane)

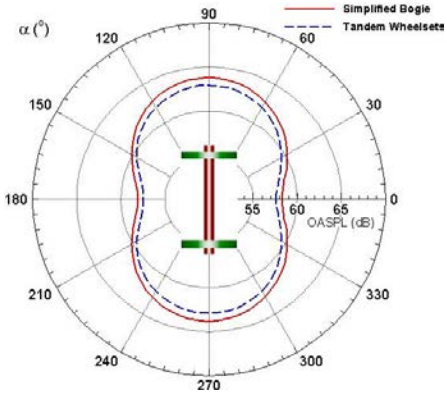

Fig. 12. Noise directivity from rear wheelset (horizontal X-Z plane)

Figs. 9 and 10 display the noise directivities from the front and rear wheelset in the vertical Y-Z plane. It can be seen that the noise level from the front or rear wheelset of the tandem wheelsets and simplified bogie are very close except at the horizontal plane through the axle centerline (α=0º or 180º) where the presence of the frame makes the difference between them (3 dB for front wheelset and 0.8 dB for rear wheelset). Compared with the front wheelset, the noise radiated from the rear wheelset is reduced by up to 9 dB except near α=0º or 180º. This is because the trailing wheelset in the turbulent flow convected from the front wheelset is

subject to a lower mean incident flow velocity. Moreover, the incident vortices impinge upon and interact with the vortices separated from the downstream wheelset, accelerating the decay of the vortex generated around it. Thus, the sound generated from periodic shedding at the rear wheelset may be lost and replaced by a broadened spectrum with a lower level. Nevertheless, in the horizontal X-Z plane, the flow separation is stronger from the downstream wheelset along the lateral side, leading to about 3 dB higher noise level than from the upstream wheelset for tandem wheelsets and slightly larger for simplified bogie.

The directivities of radiated noise from the front and rear wheelset in the horizontal X-Z plane along the flow direction are illustrated in Figs. 11 and 12. Since the frame of the bogie changes the flow behaviour around the wheelset, the noise generated from the front wheelset of the bogie is up to 4 dB higher than in the tandem wheelsets case and it is about 1 dB larger for the rear wheelset. It is interesting to note that Figs. 9 and 11 show a vertical dipole pattern of directivity for the sound radiation of the upstream wheelset, whereas Figs. 10 and 12 indicate a lateral dipole pattern of directivity from the downstream wheelset. This is due to the occurrence of laminar separation at the front wheelset and the periodic shedding which is generated at the wheelset top/bottom surface, whereas the rear wheelset is situated in a turbulent condition and large flow separation is produced along the wheelset lateral side.

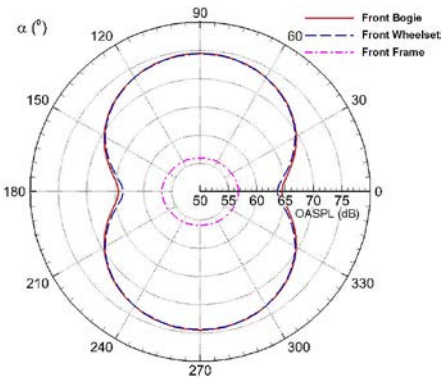

Fig. 13. Noise directivity from front bogie (vertical Y-Z plane)

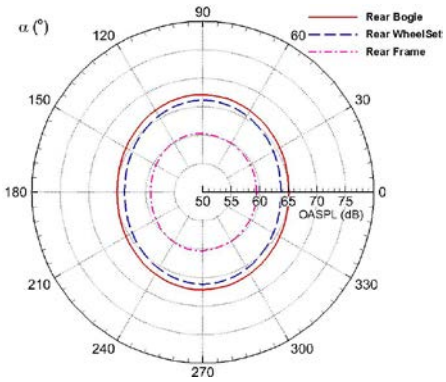

Fig. 14. Noise directivity from rear bogie (vertical Y-Z plane)

The directivities of radiated noise from the front and rear bogie in the vertical Y-Z plane are displayed in Figs. 13 and 14. Here 'front bogie' represents the upstream wheelset with the front half frame and 'rear bogie' means the downstream wheelset and the rear half frame. This demonstrates that the frames are minor sources compared to the wheelsets. The noise radiation of the rear frame is 2.5-4.5 dB larger than from the front frame because of the stronger vortex shedding and flow separation at the frame ends. Also, it can be seen that the noise radiated from the rear bogie is weaker (up to 7.3 dB) than from the front bogie except at α=0º or 180º where the noise is 0.7 dB higher from the rear bogie.

5 Conclusions

It is found that the flow past an isolated wheelset has a complex three-dimensional wake. The primary behaviour of the flow past the tandem wheelsets and the simplified bogie is that the vortices shed from the upstream bodies are convected downstream and impinge on the downstream ones, leading to the highly turbulent wake of the downstream bodies. In isolated wheelset case, the tonal noises are generated with dominant frequencies corresponding to the lift and drag dipoles due to the flow separation and vortex shedding around the axle and the wheel. Furthermore, a vertical directivity pattern of noise generation is predicted for the isolated wheelset and the front wheelset of tandem wheelsets and simplified bogie. The rear wheelset has a lateral dipole pattern of directivity and its sound radiation is generally weaker compared to the front wheelset.

In order to interpret the calculation results presented here in relation to a full scale train running at 300 km/h (83 m/s), it may be noted that the vertical dipole noise will occur at about 86 Hz and the lateral dipole at 172 Hz for the instance of isolated wheelset case with laminar inflow. The vertical dipole is likely to be significant inside the train whereas the lateral dipole noise is more important for the noise at the wayside. The noise levels will increase in proportion to the surface area (factor 100) and in proportion to the flow speed to the power of 6. In the presence of turbulent flow the tonal components are likely to be less significant and the broad-band component is likely to increase in importance. Consequently the dominance of the isolated or front wheelset in this simulation may be less pronounced. The more complex geometry in a real train will also lead to more complex flow structures and this will affect the noise radiated.

References

[1] D.J. Thompson. Railway noise and vibration: mechanisms, modelling and means of control. Elsevier, Oxford, UK, 2008.

[2] C. Talotte. Aerodynamic noise: a critical survey. Journal of Sound and Vibration, 2000, 231(3): 549–562.

[3] P.R. Spalart, M.L. Shur, M.Kh. Strelets, A.K. Travin. Initial noise predictions for rudimentary landing gear. Journal of Sound and Vibration, 2011, 330, 4180-4195.

[4] P.R. Spalart, S. Deck, M.L. Shur, K.D. Squires, M.Kh. Strelets, A.K. Travin. A new version of detached-eddy simulation, resistant to ambiguous grid densities. Theoretical and Computational Fluid Dynamics, 2006, 20:181–195.

[5] J.E. Ffowcs-Williams, D.L. Hawkings. Sound radiation from turbulence and surfaces in arbitrary motion. Philosophical Transactions of the Royal Society of London, 1969, 342: 264–321.

[6] F. Farassat. Derivation of Formulations 1 and 1A of Farassat. NASA/TM-214853, 2007.